Mapping Immune Cell Responses in Whole Blood and Solid Tumor Tissue Biopsies of Renal Cancer with CyTOF and Imaging Mass Cytometry

Nick Zabinyakov, Lauren Tracey, Ling Wang, Qanber Raza, Shakir Hasan, Michael Cohen, Nikesh Parsotam, David Howell, Liang Lim, Christina Loh

Standard BioTools Canada Inc., Markham, ON, Canada

Introduction

Immunotherapy has limited efficacy in treating solid tumor. The main hurdles include T cell exhaustion, an immunosuppressive tumor microenvironment (TME), a lack of tumor-specific antigens and a complex immune landscape. To overcome the limitation of current immunotherapies and develop novel, safe and effective treatment strategies, a comprehensive understanding of both spatially localized and systemic immune responses is essential. Multimodal analysis provides a comprehensive, holistic view of the tumor and immune environment, which is essential for accurately predicting and improving patient responses to treatment.

Materials and methods

We applied an integrative multimodal approach to map localized and systemic immune responses by employing CyTOF™ (Figure 1) and Imaging Mass Cytometry™ (IMC™) (Figure 2) technologies in matched peripheral blood mononuclear cells (PBMC), tumor-derived cells (TDCs) and formalin-fixed, paraffin-embedded (FFPE) tumor tissues from clear cell renal carcinoma (ccRCC) samples.

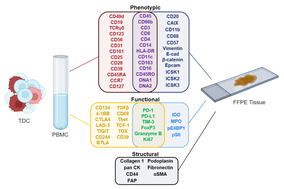

Figure 1. Antibody panels used in this study. TDC and PBMC samples were stained with a CyTOF panel, depicted in the red and yellow bubbles. FFPE tissue was stained with an IMC panel, depicted in the dark blue, light blue and **black** bubbles. Bubble overlap indicates shared markers between the CyTOF and IMC panels.

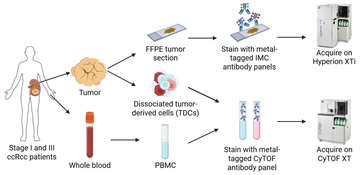

Figure 2. Workflow overview. Tumor tissue and whole blood from one Stage 1 and one Stage 3 ccRCC patient were obtained. Tumor tissue was processed in two ways: (1) FFPE tumor sections were stained with IMC antibody panels and acquired on a Hyperion™ XTi Imaging System; (2) tumor cells were enzymatically digested into dissociated TDCs. PBMC derived from the patient whole blood sample and TDCs were stained with a CyTOF antibody panel and analyzed on a CyTOF XT system.

Key takeaways

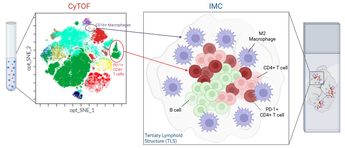

Figure 3. Deep cell profiling with CyTOF and IMC technologies. The integrated approach demonstrates the power of mass cytometry for comprehensive functional profiling of T cells and their spatial organization. These findings provide a foundation for understanding the immunological crosstalk between the peripheral immune system and the TME driving antitumor responses.

- **A multimodal approach** is paramount in understanding spatially localized and systemic immune responses. It **provides a comprehensive, holistic view** of tumor-associated phenotypes and processes.
- Deep **single-cell profiling** using a **high-parameter CyTOF panel** unveiled an **immunosuppressive TME** composed of exhausted T and NK cells and suppressed macrophages in ccRCC patients
- **In-depth T cell profiling** revealed enriched naive and cytotoxic phenotypes in PBMC, while **exhausted** TEM and TCM cells with impaired cytotoxicity dominate in the TME, along with an increased **Treg** population
- A comprehensive IMC panel revealed heterogeneous cell composition in the TME
- **Tertiary lymphoid structures** were identified in the TME and harbored exhausted CD4+ T cells. Surrounding M2 macrophages indicate significant contribution to T cell exhaustion phenotype identified by CyTOF analysis.

Results – CyTOF

Deep functional profiling with CyTOF technology reveals an immunosuppressive TME

Population frequencies visualized in high-dimensional space differ across cell types and between patients

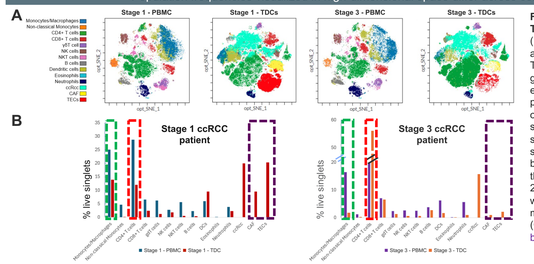

Figure 4. Cell composition differs between PBMC and TDC samples in Stage 1 and Stage 3 ccRCC patients. (Panel A) opt-SNE, a dimensionality reduction tool, was applied to live singlet cells from either PBMC samples or TDC samples and plotted. Overlaid colors correspond to gated cell populations. 73,000 events (PBMC) or 200,000 events (TDC) were proportionally sampled across two patients. Clear discrimination of major cell populations is observed. (Panel B) Quantification of gated cell subsets shown in Panel 4A represented as a percentage of total live singlets. Proportions of monocytes/macrophages are substantially decreased in TDC compared with PBMC for both patients (green box); the difference is >seven-fold for the Stage 3 patient. The proportion of CD4+ T cells is 2.8-fold higher in TDC of the Stage 3 patient compared with PBMC (red box) at the expense of monocytes/macrophages, cancer-associated fibroblasts (CAF) and tumor-associated endothelial cells (TEC; purple box).

Exhausted T and NK cells, along with suppressive macrophages, were found in the TME

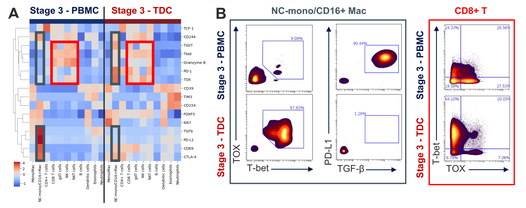

Figure 5. Exhaustion and effector phenotypes were observed in T, NK and myeloid cell subsets in Stage 3 ccRCC patients. (Panel A) Heat map of median signal intensity for each functional marker (Y-axis) across major cell populations (X-axis) in Stage 3 patient PBMC (left, blue bar) and TDC (right, red bar). Scale bar shows median intensity Z score normalized within each marker. (Panel B) Biaxial plots from non-classical (NC) monocytes/CD16+ macrophage subset (gray box) or CD8+ T cells (red box). Non-classical monocytes appear highly functional in PBMC, expressing PD-L1 and TGF-β; however, differentiated macrophages in the TME become dysfunctional and suppressed, expressing TOX and T-bet. T cells and NK cells exhibited an exhausted phenotype, particularly in TDC (less effector cytokine and upregulated PD-1/TOX).

In-depth profiling revealed exhaustive phenotype of T cells within the TME with an increased Treg population

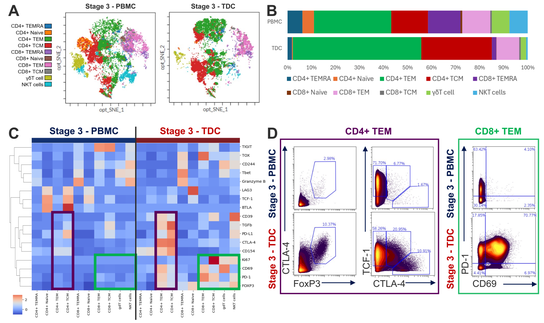

Figure 6. Profiling of systemic and local T cell subsets reveals differences in functional phenotypes in Stage 3 patient. (Panel A) opt-SNE was applied to CD3+ cells from either PBMC samples or TDC samples from the Stage 3 patient and plotted. Overlaid colors correspond to gated cell populations. 30,000 events were proportionally sampled across the two samples. Clear discrimination of major T cell populations is observed. (Panel B) Stacked bar chart quantifying the proportion of each cell subset within CD3+ T cells. Very few naive T cells are found in TDC, whereas a large increase in CD4+ TEM and TCM cells is observed compared with PBMC. (Panel C) Heat map of median signal intensity for each functional marker (Y-axis) across T cell subsets (X-axis) in Stage 3 patient PBMC (left, blue bar) and TDC (right, red bar). Scale bar shows median intensity Z score normalized within each marker. (Panel D) Biaxial plots from CD4+ TEM (purple box) or CD8+ TEM (green box) cell subsets. Overall, naive/memory phenotypes are seen in PBMC, with higher TCF-1 expression in naive and TCM T cell subsets and a more cytotoxic phenotype in CD8+ TEMRA (granzyme B+), whereas higher expression of exhaustion markers are observed in the TME in CD4 TEM/TCM subsets (for example, PD-1, CTLA-4, TOX). Within the CD4+ TEM subset, an increase in FoxP3+ Treg population was observed. Exhausted CD8+ TEM cells are found exclusively in TDC (CD69+PD-1+).

Results – Imaging Mass Cytometry

IMC analysis of ccRCC highlights the spatial distribution of functional immune cells identified by CyTOF Technology

Pixel-clustering analysis of Tissue Mode images spatially resolves major phenotypic clusters, including immune and tumor cells, and TLS

Stage 1 ccRCC, Tissue Mode IMC images (A) and pixel-clustering analysis (A')

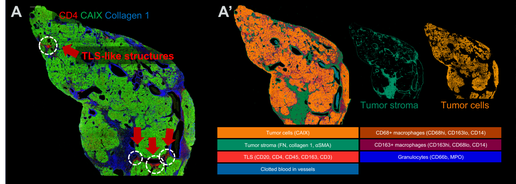

Stage 3 ccRCC, Cell Mode IMC images (B) and single-cell segmentation analysis (B')

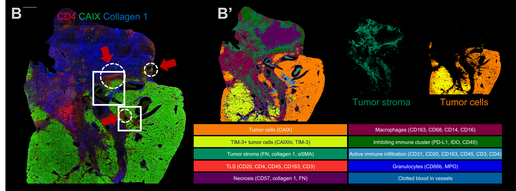

Figure 7. Visualization of the whole FFPE renal cell carcinoma tissue and unbiased pixel-clustering analysis. The whole tissue section of Stage 1 ccRCC was acquired on the Hyperion XTi Imaging System in Tissue Mode and subsequently processed with pixel-clustering analysis in MCD™ SmartViewer. Panel 7A showcases a raw composite image of selected channels with visible broad distribution of tumor cells (CAIX+) and the presence of several TLS or TLS-like structures (clusters of CD4+ cells, red arrows) in the proximity of blood vessels, suggesting presence of active immune infiltration. Pixel-clustering analysis (Panel A') revealed seven distinct clusters based on their marker expression patterns. Tumor cell cluster is the dominant cluster by area, followed by the stroma-containing cluster. TLS cluster contains multiple immune cell phenotypes including B cells, T cells and macrophages displaying an immature developmental stage. Moreover, separate subsets of macrophages include CD68+ and CD163+ cells that are sporadically distributed within the entire tumor area. Panel 7B demonstrates the whole tissue of Stage 3 ccRCC with a large component of tumor and stromal cells. Multiple TLS-like structures with mature morphologies are found within tumor cells and tumor margins. Pixel-clustering analysis (Panel 7B') identified large necrotic cluster and macrophage cluster that is concentrated in the tumor stroma. Interestingly, a subsection of tumor cells with TIM-3 expression was found, suggesting an area of potential immune evasion. Areas with TLS structures (clusters of CD4+ cells, red arrows) were chosen for further investigation in Cell Mode and single-cell segmentation analysis (see figures below). Scale bar in Panels A and B is 1 mm.

Single-cell segmentation analysis of Cell Mode images reveals a crucial role of M2 macrophages in T cell exhaustion

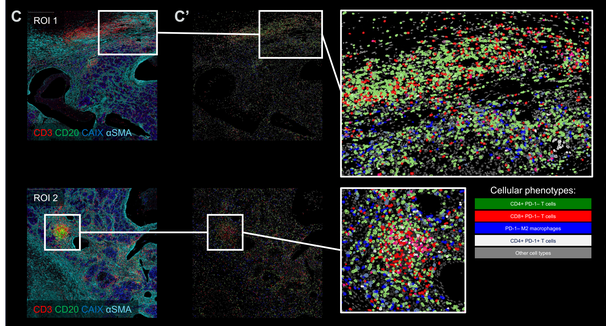

Figure 8. High-resolution visualization of regions of interest and single-cell segmentation analysis of selected phenotypes. Two ROIs from Stage 3 ccRCC containing TLS-like structures were selected and rendered using Cell Mode. Subsequent single-cell segmentation analysis conducted in QuPath defined 22,841 and 29,575 nucleated objects for ROI 1 and ROI 2, respectively. The algorithm was trained to recognize functional phenotypes of T cells and M2 macrophages. Panel C' depicts rendered composite images with spatial organization of those phenotypes. The data suggests a significant involvement of M2 macrophages in Stage 3 ccRCC. Immuno-suppressive M2 macrophages surround TLS-like structures with a small degree of penetration. The presence of CD4+ PD-1+ T cells in TLS with high proximity to M2 macrophage suggests M2 macrophages are contributing to an exhausted CD4+ T cell phenotype. ROI 1 size is 2 x 2 mm, ROI 2 – 2.5 x 2.5 mm. Scale bar is 500 µm.

Standard BioTools Inc.
2 Tower Place, Suite 2000, South San Francisco, CA 94080 USA
+1 650 266 6000 • Toll-free in the US and Canada: 866 359 4354
standardbio.com

For Research Use Only. Not for use in diagnostic procedures.
Patent and License Information: www.standardbio.com/legal/notices. Trademarks: www.standardbio.com/legal/trademarks.
Any other trademarks are the sole property of their respective owners.
©2025 Standard BioTools Inc. All rights reserved.